VERIFICATION AND VALIDATION PSEUDO-SPECTRAL FOURIER METHODOLOGY APPLIED TO TWO-PHASE FLOW

Mariana Fernandes dos Santos Villela, marianamat_ufu@yahoo.com.br
Millena Martins Villar, millena.villar@gmail.com
Aristeu da Silveira Neto, aristeus@mecanica.ufu.br
Universidade Federal de Uberlândia - UFU, Faculdade de Engenharia Mecânica - FEMEC, Laboratório de Mecânica dos Fluidos - MFLab, Av. João Naves de Avilla, 2121, Campus Santa Mônica, Bloco: 5P, Uberlândia - MG
Felipe Pamplona Mariano, fpmariano@mecanica.ufu.br
Universidade Federal de Goiás - UFG, Escola de Engenharia Elétrica e de Computação - EEEC, Av.: Universitária, 1488, Qd.: 86, Bl.: A, Setor Leste Universitário, Goiânia - GO, http://www.eee.ufg.br

Abstract.*In DNS numerical simulation of two-phases flows a high level of refinement are required when flow details and phisical discontinuity desired. Furthermore, it involves analysis of flow around complex geometries that can be moving and deforming. In order to solve these problems, in the present work numerical simulation of two phases-flow was performed using a hybrid methodology, which use Fourier pseudo-spectral coupled with Front-Tracking and Front-Capturing. This method presents high order convergence and accuracy but is limited by periodic boundary conditions. In the present work, the methodology verification is made through manufactured solution and a validation with a cylindrical rise bubble is also presented here and the terminal velocity compared with Clift* et al. *(1978) diagram.*

Keywords: *Two-phases flow, Pseudo-Spectral Fourier, Front-Tracking Method*

1. INTRODUCTION

Numerical simulations of two-phase flow require high accuracy and high convergence rate to obtain detailed information of the flow. Low computational cost is also very important, because in general, DNS require a high grid refinement, which makes them onerous. Thus, in the present work the use of Fourier pseudo-spectral to solve multiphases flow problems is proposed. This method presents high convergences rates and low computational cost, due to the algorithm named Fast Fourier Transform (FFT). Furthermore, when this method is applied to solve the Navier-Stokes equations for incompressible flows, the pressure and velocity fields are decoupled through the projection method, without the need to solve the pressure Poisson equation. To handle the two-phases flow with moving and deformable geometries, Fourier pseudo-spectral method is coupled with the Front-Tracking/ Front-Capturing method. This hybrid method use two domains, one is the Eulerian domain, where the Navier-Stokes and continuity equations are solved for the fluid and other the Lagrangian domain. For this method, both domains are coupled by interpolation and distribution process, and, the Lagrangian interface are transported through the Eulerian domain.

2. MATHEMATICAL MODELLING

2.1 Eulerian formulation

The eulerian formulation, used to describe the flow dynamic, is modeled by Navier-Stokes equations for incompressible and isothermal flows with variable in physical properties in the whole calculation domain ($\Omega = \Omega_1 \cup \Omega_2$, Fig. 1), which are given by Eqs. 1 and 2:

$$\frac{\partial u_l}{\partial t} + \frac{\partial u_l u_k}{\partial x_k} = -\frac{1}{\rho}\frac{\partial p}{\partial x_l} + \frac{1}{\rho}\frac{\partial}{\partial x_k}\left[\mu\left(\frac{\partial u_l}{\partial x_k} + \frac{\partial u_k}{\partial x_l}\right)\right] + \frac{\rho - \rho_0}{\rho} g_l + \frac{1}{\rho} f_l, \tag{1}$$

$$\frac{\partial u_k}{\partial x_k} = 0. \tag{2}$$

where ρ and μ are, respectively, the density and viscosity of the fluid, u_l is the component l of the velocity vector, p is the pressure field, f_l is the component l of the vector force field that acts on the flow at the interface, g_l is the component l of the gravitational acceleration and $l = 1, 2$, for two-dimensional problems.

The source term f_l allows the communication between the Navier-Stokes equations and the equations for interface motion. Thus, the Eulerian source term is nonzero only on the interface and zero at the rest of the Eulerian domain. This behavior is represented mathematically by the Dirac delta function (δ) (Peskin, 1977). The Eulerian force field is given by Eq.3:

$$f_l(\vec{x}, t) = \int_\Gamma F_l(\vec{X}, t)\delta(\vec{x} - \vec{X})d\vec{X}, \tag{3}$$

where $F_l(\vec{X},t)$ is the Lagrangian force in the l direction calculated on the fluid particles that compose the interface, the vector $\vec{x}$ is the position of a fluid particle on the Eulerian domain and the vector $\vec{X}$ is the position of a fluid particle which is on the interface Γ (Fig.1).

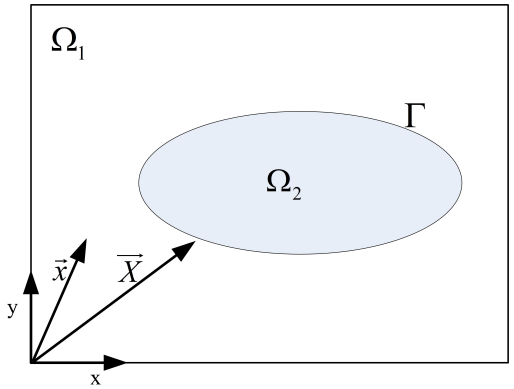

Figure 1. Definition of vectors $\vec{x}$ and $\vec{X}$.

The gravitational term, $(\rho - \rho_0)g_l$, represents the balance between the gravitacional and buoyant forces. Note that, to treat two-phase flow with periodic boundary conditions in the vertical direction (y of the Fig. 1), a restriction of this term is required in order to avoid a downward uniform acceleration throughout fluid (Esmaeeli and Tryggvason, 1999). The Eq. 4 models the ρ_0 calculation:

$$\rho_0 = (1-\alpha)\rho_c + \alpha\rho_d, \tag{4}$$

where ρ_c is the density for the continuous phase (Ω_1, Fig. 1), ρ_d is the density for the dispersed phase (Ω_2, Fig. 1) of multiphase flow and α is the volume fraction between the phases, *i.e*, is the volume fraction of dispersed phase (Ω_2, Fig. 1) by the volume of continuous phase (Ω_1, Fig. 1).

A indicator function $\Psi(\vec{x},t)$ is used to calculate the physical properties of the continuous phase, dispersed phase and the transition region between both phases. This function assumes values ranging from 0 to the continuous phase until 1 for the dispersed phase. This function $\Psi(\vec{x},t)$ is given by:

$$\Psi(\vec{x},t) = \int_\Gamma n_l(\vec{X},t)\delta(\vec{x}-\vec{X})dX_l, \tag{5}$$

where $n_l(\vec{X},t)$ is the normal vector to the interface.

With $\Psi(\vec{x},t)$ calculated at each time step, physical properties are then obtained using Eqs. 6 e 7:

$$\rho(\vec{x},t) = \rho_c + (\rho_d - \rho_c)\Psi(\vec{x},t), \tag{6}$$

$$\mu(\vec{x},t) = \mu_c + (\mu_d - \mu_c)\Psi(\vec{x},t), \tag{7}$$

where μ_c and μ_d are the viscosities of the continuous and dispersed phase, respectively.

2.2 Lagrangian formulation

The method used to tracking the interface was proposed by Unverdi and Tryggvason (1992) based on the methodology proposed by Peskin and Mcqueen (1980). In this method, the interface is defined by a Lagrangian domain which moves delimiting the dispersed phase, while the continuous phase is completely defined in the Eulerian domain. The modeling in these two domains are treated separately and the interactions between them are made by interpolation.

The calculation of Lagrangian force (Unverdi and Tryggvason, 1992) depends on the interface geometrical parameters and the pair of fluids, given by Eq.8:

$$F_l(\vec{X}) = \sigma\kappa n_l(\vec{X},t), \tag{8}$$

where σ is the coefficient of the interfacial tension $[N/m]$, κ is the curvature and n_l is the unit normal vector component.

When the interface moves due to fluid velocity or due to gravity, the new interface position can be calculated by Eq. 9:

$$\frac{\partial X_l}{\partial t} = U_l(\vec{X},t). \tag{9}$$

The Lagrangian velocity U_l is interpolated from the Eulerian velocity field, which is given by the new position X_l of the interface.

2.3 Eulerian-Lagrangean coupling

The communication between Lagrangian and Eulerian domains is done through the distribution. The distribution of interfacial Lagrangian force to Eulerian points is given by the Dirac Delta function (δ) and is represented by Eq. 3. This equation on Fourier spectral space:

$$\widehat{f}_l(\vec{k},t) = \int_\Omega e^{-ik_l.x_l} \left[\int_\Gamma F_l(\vec{X},t)\delta(\vec{x}-\vec{X})dX_l \right] dx_l. \tag{10}$$

Doing some math operations and using the definition of the Dirac delta function in Eq. 10, Eq. 11 is obtained, giving the source term of the Eulerian force in Fourier spectral space.

$$\widehat{f}_l(\vec{k},t) = \int_\Gamma F_l(\vec{X},t)e^{-ik_l.X_l}dX_l. \tag{11}$$

The indicator function (Eq. 5) on to the Fourier spectral space follows the same procedure performed for the source term and is given by Eq. 12.

$$\widehat{\Psi_l}(\vec{k},t) = \int_\Gamma n_l(\vec{X},t)e^{-ik_l.X_l}dX_l. \tag{12}$$

The Eqs. 11 and 12 were solved numerically using the Trapezium Rule (Chapra and Canale, 1985).

The interpolation function of velocity, called cubic function, proposed by Griffith and Peskin (2005), was used. This function is given by Eqs.13, 14 and 15:

$$U_l(\vec{X},t) = \sum_\Gamma D_h(\vec{X}-\vec{x})u_l(\vec{x},t)d\vec{x}_l, \tag{13}$$

$$D_h(\vec{X}-\vec{x}) = \frac{1}{h^2}W_c\left(\frac{X-x}{h}\right)W_c\left(\frac{Y-y}{h}\right), \tag{14}$$

$$W_c = \begin{cases} 1-\frac{1}{2}|r|-|r|^2-\frac{1}{2}|r|^3 & \text{if} \quad 0 \le |r| < 1 \\ 1+\frac{11}{6}|r|+|r|^2-\frac{1}{6}|r|^3 & \text{if} \quad 1 \le |r| < 2 \\ 0 & \text{if} \quad 2 \le |r| \end{cases}. \tag{15}$$

2.4 Navier-Stokes equations on a spectral Fourier space

To obtain Navier-Stokes and continuity equations, to the Fourrier space, for incompressible flows on a spectral Fourier space with periodic boundary conditions in all directions (Mariano *et al.*, 2010) (Eqs. 1 and 2), the projection method (Silveira-Neto, 2002) for the pressure-velocity decoupling is used, applying the Fourier transform properties (Briggs and Henson, 1995).

The transformation of continuity equation gives:

$$ik_k\widehat{u_k} = 0. \tag{16}$$

From the Eq.16 and the definitions coming from analytic geometry, a plan π is defined, such as it is perpendicular to the vector wave number k_l, which is contained in the vector $\widehat{u_l}(k_l,t)$ transformed, according to Fig. 2.

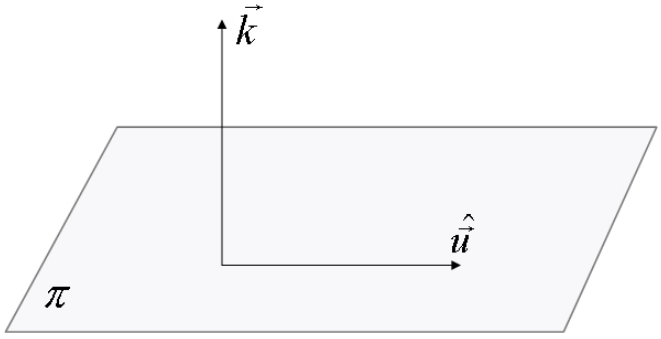

Figure 2. Definition of plan π (Silveira-Neto, 2002)

Rewritting the Eq. 1 on a spectral Fourier space, has the Eq. 17:

$$\widehat{\frac{\partial u_l}{\partial t}} + ik_k(\widehat{u_l u_k}) = \tag{17}$$
$$= -\frac{1}{\widehat{\rho}} * ik_l\widehat{p} + \frac{1}{\widehat{\rho}} * ik_k * [\widehat{\mu} * (ik_k\widehat{u_l} + ik_l\widehat{u_k})] + \frac{1}{\widehat{\rho}} * (\widehat{\rho - \rho_0})g_l + \frac{1}{\widehat{\rho}} * \widehat{f_l}.$$

Form Eq. 17, we can conclude that the rate of change of linear momentum, $\frac{\partial \widehat{u_l}}{\partial t}$, is contained in the plan π. The pressure gradient convolution product term with $\frac{1}{\widehat{\rho}}$, $\frac{1}{\widehat{\rho}} * ik_l\widehat{p}$, is colinear to the vector wave number (k_l), because $\widehat{p}$ and $\frac{1}{\widehat{\rho}}$ are scalar and thus, the convolution product $\frac{1}{\widehat{\rho}} * ik_l\widehat{p}$ is orthogonal to the plane π.

As for the advective term $ik_k(\widehat{u_l u_k})$, the source term $\frac{1}{\widehat{\rho}} * \widehat{f_l}$, the diffusive term $\frac{1}{\widehat{\rho}} * ik_k * [\widehat{\mu} * (ik_k\widehat{u_l} + ik_l\widehat{u_k})]$ and the gravitational term $\frac{1}{\widehat{\rho}} * (\widehat{\rho - \rho_0})g_l$, can not be said about their positions in relation the plan π.

Applying, then, a projection operator on the Eq. 17 (Silveira-Neto, 2002), Fig. 3, obtains the Navier-Stokes transformed to the Fourier spectral space , Eq. 18:

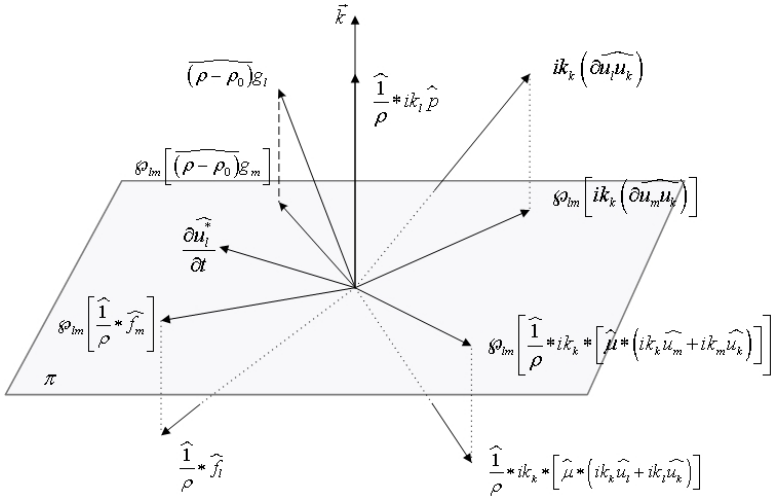

Figure 3. Projection of the source terms, advective, diffusive and gravitational term on the plan π.

$$\widehat{\frac{\partial u_l}{\partial t}} = \wp_{lm}\left[T\widehat{NL}_m - \widehat{DIF}_m - G\widehat{RAV}_m - \frac{1}{\widehat{\rho}} * \widehat{f_m}\right]. \tag{18}$$

Note by the Eq. 18 the independence of the pressure term, which was eliminated by the projection of the source term, advective, diffusive and the gravitational terms. Compared with classical schemes, this procedure is equivalent to replace the solution of a Poisson equation for a vector-matrix product what, numerically, is more computationally efficient. In physical terms, both have the same function, which ensures the mass conservation.

Despite the pressure field that do not appear in the Navier-Stokes equation, it can be retrieved for post-processing (Villela, 2011), and, after some mathematical manipulations, the pressure field is given by Eqs. 19 and 20:

$$\widehat{p} = \frac{ik_m}{k^2}\left[\widehat{\rho} * \left(T\widehat{NL}_m - \widehat{DIF}_m - G\widehat{RAV}_m - \frac{\widehat{1}}{\rho} * \widehat{f_m}\right)\right]. \tag{19}$$

where,

$$p(\vec{x}, t) = IFT[\widehat{p}(\vec{k}, t)], \tag{20}$$

IFT being the inverse Fourier transform.

3. NUMERICAL METHOD

3.1 Discrete Fourier Transform and Fast Fourier Transform

The discrete Fourier transform (DFT) given by Eq. 21, allow to work with Fourier Transform numerically.

$$\widehat{f_k} = \sum_{n=-\frac{N}{2}+1}^{\frac{N}{2}} f_n e^{\frac{-2\pi ikn}{N}}, \tag{21}$$

where k is the wave number, N is the number of grid points, n provides the position x_n placement ($x_n = n\Delta x$) and $i = \sqrt{-1}$.

The DFT transforms a function f, periodic (Figueiredo, 2007), from physical space to Fourier spectral space (Eq. 21). The Inverse Discrete Fourier Transform (IDFT) is presented by Eq. 22:

$$f_k = \frac{1}{N} \sum_{n=-\frac{N}{2}+1}^{\frac{N}{2}} \widehat{f}_n e^{\frac{2\pi i k n}{N}}. \tag{22}$$

Cooley and Tukey (1965) home developed an algorithm named Fast Fourier Transform (FFT), which solves efficiently the DFT and the IDFT (Eq. 22), what makes it attractive to solve partial differential equations using the Fourier spectral method. The disadvantage of this technique is the restriction to problems with periodic boundary conditions.

The wave numbers k_l, used in the equations transformations, are calculated as follows (Eq. 23):

$$k_{l_\eta} = \begin{cases} \eta - 1 & 1 \leq \eta \leq \frac{N}{2} + 1, \\ \eta - 1 - N & \frac{N}{2} + 2 \leq \eta \leq N. \end{cases} \tag{23}$$

where η is the position vector in a direction of the domain.

This parameter should be suited for each subroutine FFT used. In the present case, the subroutine FFTE given by Takahashi (2006), which can be found in www.ffte.jp, was used.

3.2 Treatment of non-linear term

When working with the Navier-Stokes equations using the Fourier spectral method, the resolution of non-linear term is given by a convolution integral (Briggs and Henson, 1995). Solving this integral numerically becomes impractical, then Fourier pseudo-spectral method is applied and the basic algorithm can be found at Mariano (2007).

The non-linear term can be treated in different forms (Canuto *et al.*, 1988), and have different properties when it is discretized. In the present work, a skew-symmetric form (Eq.24) is used, because of their stability:

$$\frac{1}{2}\left(\frac{\partial(u_l u_j)}{\partial x_j} + u_j \frac{\partial(u_l)}{\partial x_j}\right) \quad \texttt{or} \quad \frac{1}{2}\left(\widehat{\frac{\partial(u_l u_j)}{\partial x_j}} + u_j \widehat{\frac{\partial(u_l)}{\partial x_j}}\right). \tag{24}$$

3.3 Discretization on Force Space

As seen in subsection 2.2, Lagrangian force density is depend on interface curvature, κ_l and the unit normal vector n_l. The discretizations of the vector n_l and the κ_l are made using the Lagrange polynomials (Villar *et al.*, 2010).

3.4 Time discretization

It's necessary to use a time advance methodology that is compatible with the high accuracy of the spectral methodology applied in the space. The best results are obtained with the of optimized Runge Kutta time advancement method (RK46). This method is an explicit method of fourth order and six stages. The algorithm is given by Allampalli *et al.* (2009).

3.5 Filtering Process

Another important procedure is the need to filter all the terms on the right side of the Navier-Stokes equations due to the discontinuities generated by the forcing term, which shows abrupt changes in physical properties. These discontinuities generate the Gibbs phenomenon (Navarra, 1994), and with the filter process, tends to disappear leading to increased order. The filtering process is given by Eq. 25:

$$\widehat{f}(\vec{k}, t)_{filtrado} = \varphi(\theta)\widehat{f}(\vec{k}, t), \tag{25}$$

where $\varphi(\theta)$ is the filter function.

In the present work the filter used is the "Raised Cosine". Its mathematical model can be found at Mariano *et al.* (2010).

4. RESULTS

4.1 Numerical verification

The verification performed in this work is done through the technique of manufactured solutions, where a source term is introduced in differential equations, creating a mathematical problem that has an analytical solution.

Here the Navier-Stokes equations are verified, where the gravitational term is not considered. In this way the f_l term is determined by analytical solution. The Navier-Stokes equations has the following form:

$$\rho\left[\frac{\partial u_l}{\partial t}+\frac{\partial u_l u_k}{\partial x_k}\right]=-\frac{\partial p}{\partial x_l}+\left(\frac{\partial}{\partial x_k}\left[\mu\left(\frac{\partial u_l}{\partial x_k}+\frac{\partial u_k}{\partial x_l}\right)\right]\right)+f_l, \tag{26}$$

where the forcing term f_l obtained from the analytical equations presented by Nós (2007), u and v being the velocity fields in horizontal and vertical directions, respectively and p is the pressure field.

The analytical solutions to u, v and p are given by Eq. 27. The superindex e stands for the or exact analytical solutions, in which $(x, y) = x_l \in [0, 1] \times [0, 1]$. The initial conditions are given by $u(0, x) = u^e(0, x)$, $v(0, x) = v^e(0, x)$, ρ^e is the analytical density and μ^e is the analytical dynamic viscosity.

$$u^e(x,t) = sin^2(2\pi x + 2\pi y + t), \tag{27}$$
$$v^e(x,t) = cos^2(2\pi x + 2\pi y + t), \tag{28}$$
$$p^e(x,t) = cos(2\pi x + 2\pi y + t). \tag{29}$$

To verify the implementation of the Navier-Stokes equations, with variable physical properties, the density (ρ_e) and the viscosity (μ_e) are given by:

$$\rho_e(x,t) = 1 + 0,1[sin^2(2\pi x + 2\pi y + t)], \tag{30}$$
$$\mu_e(x,t) = 1 + 0,2[cos^2(2\pi x + 2\pi y + t)]. \tag{31}$$

The Tab. 1 shows the results of the norm L_2 of the error, obtained on an uniform grid and periodic boundary conditions, as previously described.

Table 1. Norm L_2 for u, v and p errors with ρ and μ variables $t = 5[s]$.

Mesh	Variable	Norm L_2
32×32	u	$5,3265 \times 10^{-15}$
	v	$5,3222 \times 10^{-15}$
	p	$3,9150 \times 10^{-15}$
64×64	u	$1,5811 \times 10^{-15}$
	v	$1,5637 \times 10^{-15}$
	p	$2,7136 \times 10^{-15}$
128×128	u	$1,1230 \times 10^{-15}$
	v	$1,1084 \times 10^{-15}$
	p	$2,9079 \times 10^{-15}$

The Tab. 1 shows that the error, given by the norm L_2, atain machine error, when double precision is used. Comparing with Nós (2007) work, the present work presents high accuracy with Fourier pseudo-spectral method when working with varables physical properties, than Nós (2007). This author report an errors on the 10^{-2} order to a grid $128 \times 128 \times 128$.

4.2 Cylindrical buble rise

In the present work a rise bubble in two-dimensional domain, was simulated. This study consider that the fluid are initially at rest and have periodic boundary conditions in both directions.

The result is compared with by experimental data provided by Clift *et al.* (1978) diagram, where for different numbers of Eötvös and Morton (Villela, 2011), this diagram provides the Reynolds number and different shapes. So, is possible to compare the bubble shape and the Reynolds number to validate the process.

For all tests presented, the domain was given by $\Omega = [0; 4\pi] \times [0; 12\pi]$, the surface tension σ is 1.0 $[N/m]$, the bubble diameter d_d $[m]$ is 0.7π $[m]$, the mesh is 128×384 and a $\delta t = 0.001$ $[s]$. The dimensionless coordinates x and y were obtained using the bubble diameter and the dimensionless time given by $t^* = \frac{t}{\sqrt{d_d/g}}$.

Two other parameters models the flow of a rise bubble, which are the density ratios λ and the viscosity ratios γ (Villela, 2011). For the simulations presented here a fixed density e viscosity ratio of 0.5 is used.

The Eötvös and Morton numbers assumes values equal to 1 and 0.01, respectively. For those parameters the bubble presents a cylindrical shapes. Fig. 4, shows the density field evolution.

A second case is simulated and showed in Fig. 5 where the density field of a rise bubble deformed is presented. Through the diagram of Clift *et al.* (1978) the Eötvös and the Morton number are used in the present work, $E_o = 100$ and $M = 1000$. For these values the bubble must atain an ellipsoidal-cap. The Reynolds number assumes $Re = 1$.

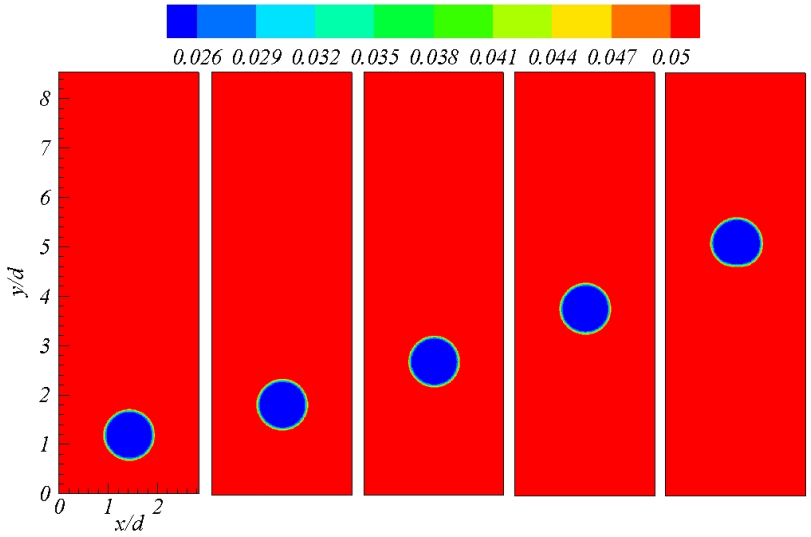

Figure 4. Temporal evolution of the density field for $Eo = 1$ and $M = 0.01$.

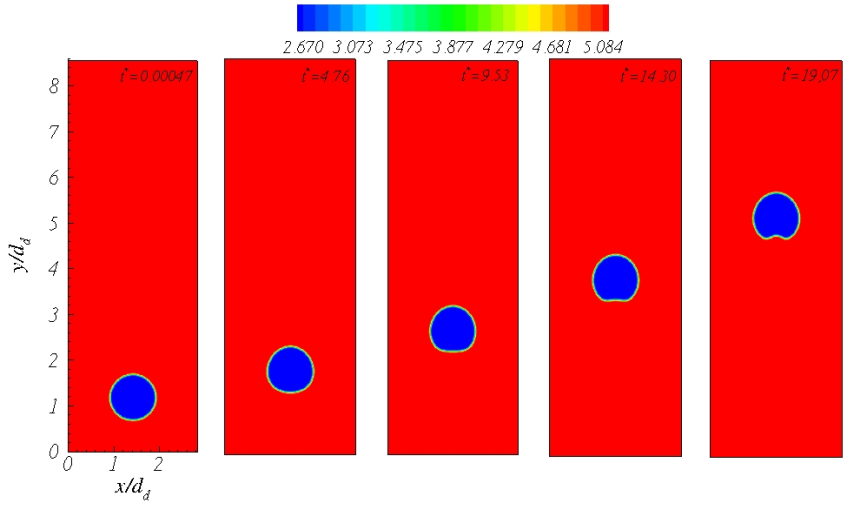

Figure 5. Temporal evolution of the field of density for $Eo = 100$ and $M = 10.000$

5. CONCLUSIONS

In the present work numerical simulations of two-phase flow using the Fourier pseudo-spectral methodology coupled with the hybrid method Front-Tracking/Front-Capturing are presented. The numerical code for physical variables properties ρ and μ, is verified through the manufactured technique where it reaches machine error. The manufacturing solution used here is adapted from Nós (2007), which presented errors of order of 10^{-2} for the refined mesh. Although the proposed methodology reached high accuracy on the error analysis.

Flows with rising cylindrical and cap-ellipsoidal bubbles, are presented in the present work. The preliminary results for rising bubbles are consistent with the physics presented by others authors.

6. ACKNOWLEDGEMENTS

The authors thank the College of Mechanical Engineering (FEMEC) of the Federal University of Uberlândia (UFU), Capes, FAPEMIG and CNPq for financial support.

7. REFERENCES

Allampalli, V., Hixon, R., Nallasamy, M. and Sawyer, S., 2009. "High-accuracy large-step explicit runge - kutta ($hale - rk$) schemes for computational aeroacoustics". *Journal of Computational Physics*, Vol. 228.

Briggs, W.L. and Henson, V.E., 1995. *DFT*. Philadelphia: SIAM.

Canuto, C., Hussaini, M., Quarteroni, A. and Zang, T., 1988. *Spectral methods in fluid dynamics*. New York: Springer-

Verlag.

Chapra, S. and Canale, R., 1985. *Numerical Methods for Engineers*. McGraw-Hill.

Clift, R., Grace, J.R. and Weber, M.E., 1978. *Bubles, Drops and Particles*. Academic Press, London.

Cooley, T.W. and Tukey, J.W., 1965. "An algorithm for the machine calculation of complex fourier series". *Mathematics Computations*, Vol. 19, pp. 297–301.

Esmaeeli, A. and Tryggvason, G., 1999. "Direct numerical simulations of bubbly flows part 2. moderate reynolds number arrarys". *Journal of Fluid Mechanics*, Vol. 385, pp. 325–358.

Figueiredo, G., 2007. *Análise de Fourier e Equações Diferenciais Parciais*. IMPA-Rio de Janeiro.

Griffith, B.E. and Peskin, C.S., 2005. "On the order of accuracy of the immersed boundary method: Higher order convergence rates for sufficiently smooth problems". *Journal of Computational Physics*, Vol. 37, pp. 75–105.

Mariano, F., 2007. *Simulação de Escoamentos Não-Periódicos Utilizando as Metodologias Pseudo-Espectral de Fouriere da Fronteira-Imersa*. Universidade Federal de Uberlândia-Faculdade de engenharia Mecânica.

Mariano, F., Moreira, L., Silveira-Neto, A., Silva, C. and Pereira, J., 2010. "A new incompressible navier-stokes solver combining fourier pseudo-spectral and immersed boundary methods". *Computer Modeling Engineering and Sciences*, Vol. 59, pp. 181–216.

Navarra, A., 1994. "Reduction of the gibbs oscillation in spectral model simulation". *Journal of Climate*, Vol. 7, pp. 1169–1183.

Nós, R.L., 2007. *Simulações de escoamentos tridimensionais bifásicos empregando métodos adaptativos e modelos de campo de fase.* Ph.D. thesis, Universidade de São Paulo, São Paulo.

Peskin, C.S., 1977. "Numerical analysis of blood flow in the heart". *Jounal of Computatinonal Physics*, Vol. 25, p. 220.

Peskin, C.S. and Mcqueen, D.M., 1980. "Modeling prosthetic heart valves for numerical analysis of blood flow in the heart". *Journal of Computational Physics*, Vol. 37.

Silveira-Neto, A., 2002. *Apostila da Disciplina Mecânica dos Fluidos do Programa de Pós-Graduação da Universidade Federal de Uberlândia*. Uberlândia: UFU.

Takahashi, D., 2006. "A hybrid mpi/openmp implementation of a parallel 3-d fft on smp clusters". *Proc. 6th International Conference on Parallel Processing and Applied Mathematics (PPAM 2005), Lecture Notes in Computer Science*, Vol. 3911, pp. 970–977.

Unverdi, S.O. and Tryggvason, G., 1992. "A front-tracking method for viscous, incompressible, multifluid flows". *Journal of Computational Physics*, Vol. 100, pp. 25–37.

Villar, M., Ceniceros, H., Roma, A. and Silveira-Neto, A., 2010. "A robust, fully adaptive hybrid level-set/front-tracking method for two phase flows with an accurate surface tension computation". *Communication in Computer Physics*, Vol. 8, pp. 51–94.

Villela, M.S., 2011. *MODELAGEM MATEMÁTICA DE ESCOAMENTOS BIFÁSICOS USANDO O MÉTODO ESPECTRAL DE FOURIER*. Universidade Federal de Uberlândia-Faculdade de engenharia Mecânica.

8. Responsibility notice

The authors are the only responsible for the printed material included in this paper